

Precision measurement of the ground-state hyperfine constant of $^{25}\text{Mg}^+$

Wayne M. Itano and D. J. Wineland

Time and Frequency Division, National Bureau of Standards, Boulder, Colorado 80303

(Received 13 April 1981)

The ground-state hyperfine constant A and the nuclear-to-electronic g -factor ratio g_I/g_J of $^{25}\text{Mg}^+$ have been measured by a laser optical-pumping double-resonance technique. The ions were stored in a Penning trap at a magnetic field of about 1 T. The results are $A = -596.254\,376(54)$ MHz and $g_I/g_J = 9.299\,484(75) \times 10^{-5}$. The magnetic field at the ions was stabilized by servoing it to an ($\Delta m_I = 0$, $\Delta m_J = \pm 1$) electronic Zeeman transition. Other hyperfine ($\Delta m_I = \pm 1$, $\Delta m_J = 0$) transitions were detected while the field was thus stabilized. The derivative of the (m_I, m_J) = ($-3/2, 1/2$) to ($-1/2, 1/2$) transition frequency with respect to magnetic field B_0 goes to zero at $B_0 \approx 1.24$ T. The corresponding resonance was observed at this field with linewidths as small as 0.012 Hz ($Q = 2.4 \times 10^{10}$) by implementing the Ramsey interference method with two coherent rf pulses separated in time by up to 41.4 s.

I. INTRODUCTION

The ground-state magnetic-dipole hyperfine constants (A values) of the neutral alkali atoms have been measured to high precision by optical-pumping and atomic beam magnetic resonance techniques.^{1,2} A variety of theoretical methods have been used to calculate these quantities.³ By comparison, much less experimental and theoretical work has been done on the singly ionized alkaline-earth atoms, which are isoelectronic to the alkalis. Purely optical measurements generally suffer from low resolution. Direct and indirect optical-pumping methods have been used to measure the ground-state A values of several alkaline-earth ions and some other ions that have a $^2S_{1/2}$ ground state,⁴ either in buffer-gas cells [Ba^+ , Cd^+ , Be^+ , Mg^+ (Ref. 5)] or in ion traps [He^+ , Hg^+ (Ref. 6), Ba^+ (Ref. 7)]. Also, electron-spin resonance (ESR) spectroscopy has been used to study Mg^+ (Ref. 8) and Cd^+ (Ref. 9) trapped in solid rare-gas matrices, where the A values may be shifted from their free-ion values by a significant amount. This shift is typically a few percent for the neutral alkalis.¹⁰ The ground-state A value of Li-like fluorine has been measured by the method of perturbed angular correlations.¹¹ A few calculations of the ground-state A values of alkali-like positive ions have been published, especially for the Li series.^{3,12}

In this paper, we report on the first high-precision determination of the ground-state A value of the free $^{25}\text{Mg}^+$ ion. The nuclear-to-electronic g -factor ratio g_I/g_J was also determined. A preliminary report on these measurements has appeared previously.¹³

Our experimental techniques have several unusual features:

(1) The ions were stored in a Penning ion trap in ultrahigh vacuum. Perturbations to energy

levels caused by collisions with neutral molecules or other ions or by the trapping fields were very small, except for the Zeeman shift due to the large applied magnetic field. Relaxation times were many seconds so that very narrow resonances could be observed.

(2) Resonant light pressure from a frequency-doubled dye laser was used to reduce the ion temperature to less than 1 K, thus reducing all Doppler effects, and to confine the ions to a small volume around the trap center, which reduced magnetic-field inhomogeneity effects.¹⁴⁻¹⁸

(3) Laser optical-pumping, double-resonance techniques can achieve good signal-to-noise ratios, even with very small ion numbers.¹⁷ In fact, double-resonance signals can be observed from a single ion.^{14,18}

(4) The experiments were carried out in a high magnetic field, which was needed to confine the ions. In this case, the transition frequencies depend upon A , the g factors, and the magnetic field. Short-term fluctuations (~ 1 s) of the magnetic field imposed the main limitation on the determinations of A and g_I/g_J .

The details of the experimental method are discussed in Sec. II. The values of A and g_I/g_J are calculated from the data and their uncertainties are estimated in Sec. III. In Sec. IV these values are compared with the results of other experiments and with theory, and applications and extensions of our experimental techniques are discussed.

II. EXPERIMENTAL METHOD

A. $^{25}\text{Mg}^+$ level structure

Singly ionized Mg is isoelectronic to neutral Na. The ground state is labeled $3s\,^2S_{1/2}$, and the first excited states are labeled $3p\,^2P_J$ ($J = \frac{1}{2}, \frac{3}{2}$). Light of wavelength 279.6 nm was used to drive the

transition from the ground state to the $3p^2P_{3/2}$ level. The ^{25}Mg nucleus has nuclear spin $I = \frac{5}{2}$, so the ground and excited states have hyperfine structure. The experiments were carried out in a magnetic field of about 1 T, so that the nuclear and electronic angular momenta \vec{I} and \vec{J} were essentially decoupled. Figure 1 shows the ground-state energy levels as a function of magnetic field. The hyperfine constants of the $3p^2P_{3/2}$ state have not been measured. However, they can be estimated¹⁹ from the known $3p^2P_J$ fine structure splitting²⁰ and the known magnetic dipole²¹ and electric quadrupole²² moments of the ^{25}Mg nucleus. These values are $A \approx -18$ MHz and $B \approx 22$ MHz. A value for the effective nuclear charge $Z_i = 10$ was assumed.

B. Apparatus

The basic experimental apparatus has been described previously.^{15,16} A Penning-style ion trap, which uses a uniform magnetic field and a quadrupolar electrostatic potential,²³ was used to store the ions. The characteristic dimensions of the trap were $r_0 = 1.64z_0 = 0.63$ cm. Typical operating parameters were $V_0 = 7$ V and $B_0 = 1$ T. $^{25}\text{Mg}^+$ ions were loaded into the trap in the following way: An electron beam coincident with the trap axis created positive ions by collisions with background gas, which were confined by the trap. An oven containing ^{25}Mg of 98% isotopic purity was heated, and the ^{25}Mg neutrals underwent charge-exchange reactions with the trapped positive ions to yield trapped $^{25}\text{Mg}^+$ ions. The magnetron radii of the ions

increased slowly due to collisions with background gas. The storage time has been observed to be about one day without light pressure cooling or confinement. The number of ions initially stored could be varied from about 10^4 down to about one by varying the current and duration of the electron beam. Typical numbers for the experiments reported here were about 10 to 100 ions. The reason for using such small numbers was that in order to get experimentally convenient optical-pumping time constants of no more than a few seconds, relatively high light intensity was required. Since the total available power was low (< 40 μW), it was necessary to focus the beam to a small spot size (about $50\text{-}\mu\text{m}$ diameter). The maximum ion density is limited by space-charge effects, so in order for the ion cloud to be small enough to have good overlap with the focused beam, the total ion number had to be small. During the resonance experiments, the background pressure was maintained below 1.3×10^{-7} Pa (10^{-9} Torr).

The source of 279.6 nm radiation was the second harmonic of the output of a single-mode cw rhodamine 110 dye laser. The frequency doubling took place in a 90° -phase-matched AD^*P (deuterated ammonium dihydrogen phosphate) crystal, operated at a temperature of about 117°C . The uv power generated was typically between 5 and 30 μW . The bandwidth of the dye laser was about 1 MHz and could be frequency stabilized in a long term to about ± 200 kHz by locking it to a saturated absorption hyperfine feature in I_2 . If the laser frequency was fixed in this way, fine tuning could be accomplished by varying the trap magnetic field to Zeeman shift the Mg^+ levels.

The second harmonic radiation was separated from the fundamental by a prism and focused into the trap, passing through 3-mm holes drilled into the ring electrode. The beam entered and exited from the vacuum enclosure through Brewster-angle windows. Resonance fluorescence photons emitted into the backward direction inside an $f/4$ cone were collected by a flat mirror set at 45° to the incident beam and imaged by lenses onto a photomultiplier tube (PMT). (The incident beam passed through a hole in this mirror.) Two stages of spatial filtering were used to reduce background due to light scattered from the windows. An interference filter centered at 280 nm and a Corning 7-54 glass filter reduced background due to light at other wavelengths. The net detection efficiency for a photon emitted from an ion, taking into account the detection solid angle, mirror reflectivity, transmission of the lenses and filters, and PMT quantum efficiency, was about 2×10^{-5} .

Data collection was controlled by a minicomputer, which swept the rf or microwave frequency

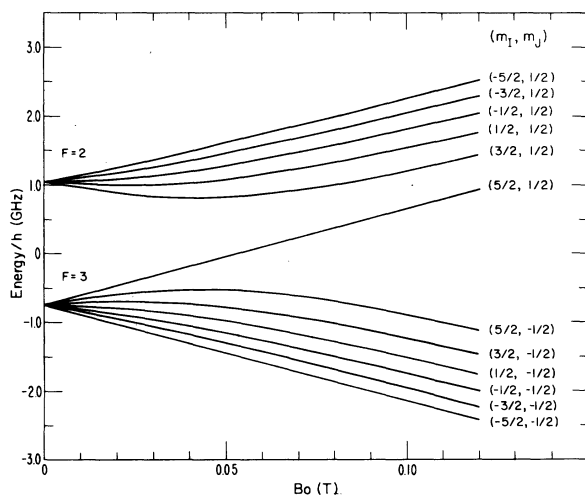


FIG. 1. Ground-state energy levels of $^{25}\text{Mg}^+$ as a function of the magnetic field B_0 . Note the transition from low field, where \vec{I} and \vec{J} are coupled to form the total angular momentum \vec{F} , to high field, where they are decoupled. All of the experiments were done at high field.

used to drive the $^{25}\text{Mg}^+$ ground-state transitions and recorded the number of photons detected by the PMT. The output of various frequency synthesizers was applied to a probe near the gap between the endcap and ring electrode and used to drive the nuclear spin flip ($\Delta m_J = 0$, $\Delta m_I = \pm 1$) rf transitions at about 300 MHz. The output of a klystron was directed at the trap from the end of a waveguide positioned outside one of the Brewster windows and used to drive the electronic spin flip ($\Delta m_J = \pm 1$, $\Delta m_I = 0$) microwave transitions at about 30 GHz. The klystron was phase locked to the third harmonic of a microwave frequency synthesizer. For high-accuracy work, the frequency synthesizers were phase locked to the output of a cesium atomic beam frequency standard. The computer also controlled an rf switch and a light shutter, which were necessary for some of the resonance schemes.

C. Resonance methods

The basic principles of the optical-pumping, double-resonance methods have been outlined previously.¹⁷ Resonant light pressure was used to cool the ions to roughly 1 K and to confine them to a small volume near the trap center. The electronic Zeeman splitting was much greater than the Doppler width. With light polarized perpendicular to the magnetic field and slightly lower in frequency than the ($^2S_{1/2}$, $m_I = -\frac{5}{2}$, $m_J = -\frac{1}{2}$) to ($^2P_{3/2}$, $m_I = -\frac{5}{2}$, $m_J = -\frac{3}{2}$) transition frequency, the steady-state population of the ($^2S_{1/2}$, $m_I = -\frac{5}{2}$, $m_J = -\frac{1}{2}$) level was about 94% and the ($^2S_{1/2}$, $m_I = -\frac{5}{2}$, $m_J = \frac{1}{2}$) population was about 6%, as a result of competition between relatively weak off-resonance transition rates.¹⁷ The frequency detuning from the resonance center, typically about 30 to 50 MHz, was necessary in order to provide cooling.^{14,15} At the light intensities used, these weak pumping rates were about 1 s^{-1} , much faster than any other relaxation rate between ground-state sublevels.

The optical-pumping mechanism is unusual in that the ($m_I = -\frac{5}{2}$, $m_J = -\frac{1}{2}$) ground-state sublevel, which is driven to the excited state at the highest rate, retains the highest steady-state population. The optical transition frequencies are shown in Fig. 2. Optical pumping into the $m_J = -\frac{1}{2}$ ground-state manifold takes place by the same mechanism as for $^{24}\text{Mg}^+$, which has zero nuclear spin. The m_I quantum number can be ignored for this part of the discussion. For light polarized perpendicular to the magnetic field, m_J must change by ± 1 in a transition from the ground state to the excited state. In spontaneous decay from the excited state to the ground state, m_J can change by 0 or ± 1 . Thus, the $-\frac{1}{2} \rightarrow -\frac{3}{2}$ transition, which is strongly driven by the laser, and the $+\frac{1}{2} \rightarrow \frac{3}{2}$ tran-

sition do not optically pump the ground state. The first and second numbers refer to the ground- and excited-state m_J values. The other allowed transitions, $+\frac{1}{2} \rightarrow -\frac{1}{2}$ and $-\frac{1}{2} \rightarrow +\frac{1}{2}$, do cause optical pumping because the ion can decay to either ground-state m_J manifold. These transitions are driven weakly in their Lorentzian wings. Since the second harmonic of the laser frequency is close to the $-\frac{1}{2} \rightarrow -\frac{3}{2}$ transition frequency, its detuning from the $-\frac{1}{2} \rightarrow +\frac{1}{2}$ transition is four times as great as its detuning from the $+\frac{1}{2} \rightarrow -\frac{1}{2}$ transition (see Fig. 2). Hence, the $m_J = +\frac{1}{2}$ ground-state manifold is depopulated 16 times faster than the $m_J = -\frac{1}{2}$ manifold. In the steady state, the $m_J = -\frac{1}{2}$ manifold has 16 times the population of the $m_J = +\frac{1}{2}$ manifold, provided that the optical-pumping rate is much faster than competing relaxation rates. Optical pumping into the ($m_I = -\frac{5}{2}$) ground-state sublevels occurs because of hyperfine coupling in the excited state. The excited-state sublevels, which are labeled (m_I , $m_J = -\frac{3}{2}$), actually contain small admixtures of states with lower m_I , except for ($m_I = -\frac{5}{2}$, $m_J = -\frac{3}{2}$), which is pure. For example, the state which is nominally ($m_I = -\frac{3}{2}$, $m_J = -\frac{3}{2}$) contains a small amplitude (about 1.4×10^{-3} at $B_0 = 1 \text{ T}$) of the $m_I = -\frac{5}{2}$, $m_J = -\frac{1}{2}$ state, etc. Hence, if an ion in the (m_I , $m_J = \frac{1}{2}$) ground-state sublevel is driven to the (m_I , $m_J = -\frac{3}{2}$) excited-state sublevel, it has a small probability of decaying to a ground-state sublevel with lower m_I , unless $m_I = -\frac{5}{2}$. Eventually, the ions are trapped in the $m_I = -\frac{5}{2}$ sublevels. The process by which an ion absorbs and emits a photon and is left in a different ground-state sublevel has been treated as if the absorption and emission were separate events. It would be more accurate to describe this process in terms of spontaneous resonance Raman scattering, but this distinction is actually of no importance, since neither the coherence nor the time delay between the two events is of interest.

The fluorescence level was proportional to the ($^2S_{1/2}$, $m_I = -\frac{5}{2}$, $m_J = -\frac{1}{2}$) population. Hence, a transition which changed this population could be detected as a change in fluorescence. In the following, let the ($^2S_{1/2}$, m_I , m_J) state be denoted by (m_I , m_J). Both the ($-\frac{5}{2}$, $-\frac{1}{2}$) to ($-\frac{3}{2}$, $-\frac{1}{2}$) nuclear spin-flip transition and the ($-\frac{3}{2}$, $-\frac{1}{2}$) to ($-\frac{5}{2}$, $\frac{1}{2}$) electronic spin-flip transition were detected by a decrease in fluorescence when rf at the resonance frequency was applied. When the rf transition was saturated, the fluorescence dropped by about 50%. This technique was previously used to detect the ground-state electronic spin-flip transition of $^{24}\text{Mg}^+$, which has zero nuclear spin.¹⁷ When light was tuned close to the ($^2S_{1/2}$, $m_I = \frac{5}{2}$, $m_J = \frac{1}{2}$) to ($^2P_{3/2}$, $m_I = \frac{5}{2}$, $m_J = \frac{3}{2}$) transition, most of the population was pumped into the ($\frac{5}{2}$, $\frac{1}{2}$) state. The ($\frac{5}{2}$,

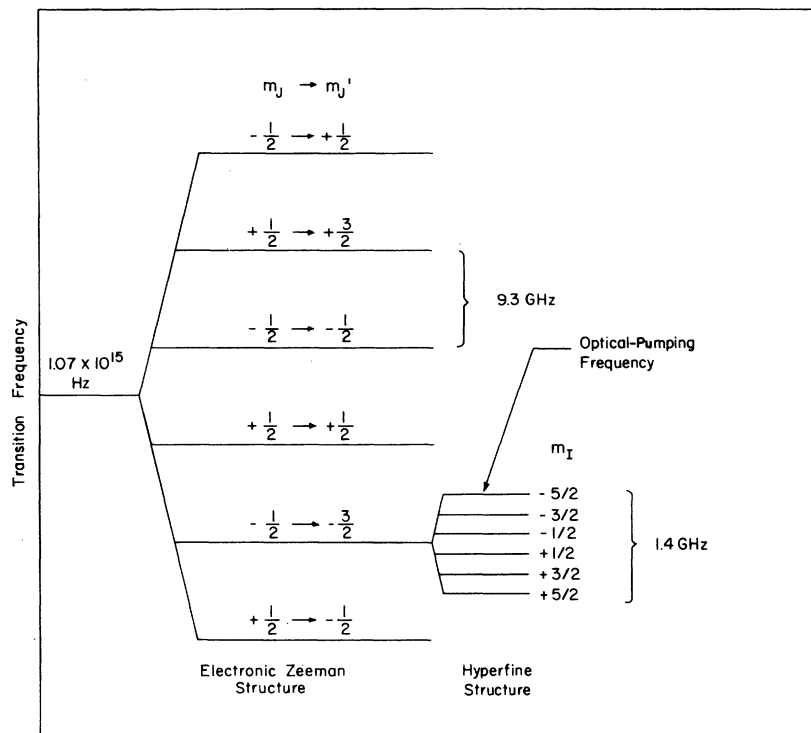


FIG. 2. Structure of the $^{25}\text{Mg}^+ 3s\ ^2S_{1/2}$ to $3p\ ^2P_{3/2}$ 279.6-nm line at a magnetic field $B_0 = 1$ T. The quantum numbers m_J and m_J' refer to the ground and excited states, respectively. The frequency splitting between adjacent electronic Zeeman components is approximately $\frac{2}{3}\mu_B B_0/h$. At high magnetic field, m_I is a good quantum number which is conserved in the optical transition process. Hence, each electronic Zeeman component splits into six hyperfine components corresponding to different values of m_I . This splitting is shown for the $(m_J \rightarrow m_J') = (-\frac{1}{2} \rightarrow -\frac{3}{2})$ component. The hyperfine splitting is drawn to a different scale than the electronic Zeeman splitting. The natural linewidth is 43 MHz, and the Doppler width is typically 100 MHz when the ions are cold. For most of the optical pumping experiments, the laser was tuned so that its second harmonic was about 30 to 50 MHz lower than the $(^2S_{1/2}, m_I = -\frac{5}{2}, m_J = -\frac{1}{2})$ to $(^2P_{3/2}, m_I = -\frac{5}{2}, m_J = -\frac{3}{2})$ transition, which is marked with an arrow.

$\frac{1}{2}$) to $(\frac{3}{2}, \frac{1}{2})$ and $(\frac{5}{2}, \frac{1}{2})$ to $(\frac{5}{2}, -\frac{1}{2})$ transitions were then detected by a decrease in fluorescence when rf was applied.

Other transitions were detected by more complex resonance schemes. The $(-\frac{5}{2}, \frac{1}{2})$ to $(-\frac{3}{2}, \frac{1}{2})$ transition was detected by a triple resonance method. The ions were optically pumped into the $(-\frac{5}{2}, -\frac{1}{2})$ state, the $(-\frac{5}{2}, -\frac{1}{2})$ to $(-\frac{5}{2}, \frac{1}{2})$ transition was saturated by frequency modulating the klystron through the resonance at a rate of about 10 Hz, and a decrease in fluorescence was observed as a frequency synthesizer was swept through the $(-\frac{5}{2}, \frac{1}{2})$ to $(-\frac{3}{2}, \frac{1}{2})$ resonance. The $(-\frac{3}{2}, \frac{1}{2})$ to $(-\frac{1}{2}, \frac{1}{2})$ transition was also detected by a quadruple resonance method. The ions were optically pumped into the $(-\frac{5}{2}, -\frac{1}{2})$ state and both the $(-\frac{5}{2}, -\frac{1}{2})$ to $(-\frac{5}{2}, \frac{1}{2})$ transition and the $(-\frac{5}{2}, \frac{1}{2})$ to $(-\frac{3}{2}, \frac{1}{2})$ transition were saturated. A decrease in fluorescence was observed as the frequency of another oscillator was swept through the $(-\frac{3}{2}, \frac{1}{2})$ to $(-\frac{1}{2}, \frac{1}{2})$ resonance. The reason for going to such lengths to observe this transition is that the first derivative

of its frequency with respect to magnetic field goes to zero at about 1.24 T, so that broadening and shifts of the resonance due to magnetic-field instability are essentially eliminated. The $(-\frac{5}{2}, \frac{1}{2})$ to $(-\frac{3}{2}, \frac{1}{2})$ transition frequency becomes field independent at about 1.9 T, which was higher than our electromagnet could reach. These methods could be extended to observe other transitions with further reduction in signal.

D. Resonance shifts and broadenings

The rf and microwave resonances can be broadened and shifted by magnetic-field fluctuations and drift and by interaction with the uv radiation and with additional rf fields. At $T = 20$ K, which was higher than was reached in any of the resonance experiments, the fractional frequency shift due to the second-order Doppler effect is -1.1×10^{-13} , which is negligible. Frequency shifts due to collisions with ions and neutral molecules were also negligible. At low temperatures, the repulsive

Coulomb force kept positive ions from approaching each other very closely. At a temperature T , the distance of closest approach R is given roughly by $k_B T = e^2/R$. For $T = 20$ K, $R = 8.4 \times 10^{-5}$ cm, so that spin exchange reactions between ions did not occur. The maximum electric field for this case is $e/R^2 = 21$ V/cm, and the rms field is much lower, so Stark shifts of the hyperfine structure are too small to be observable. Electrons and negative ions were expelled from the Penning trap because the potentials were set to trap positive ions. Collisions with background neutrals took place at a rate of less than about $(5 \text{ min})^{-1}$, which was determined from the ion temperature relaxation rate. Spin depolarization rates, which would increase the resonance linewidths, should be much lower.⁴ Fractional hyperfine density (pressure) shifts, estimated from the known shift for the $^{137}\text{Ba}^+$ ion,⁴ were less than 10^{-15} .

In general, the magnetic-field instability caused the greatest uncertainty in determining the resonance frequencies. The fractional fluctuations, measured with an NMR probe, were about 2×10^{-7} in 1 s and 10^{-6} in several seconds, with occasional sudden jumps of about 10^{-6} . The electronic spin-flip transition frequencies are essentially proportional to the magnetic field B_0 , so that typically, a 10^{-6} shift in B_0 causes a 30 kHz frequency shift at 30 GHz. The nuclear spin-flip transition frequencies have field sensitivities that vary with B_0 . A 10^{-6} shift in B_0 at $B_0 = 1.14$ T causes a 16-Hz shift of the $(-\frac{5}{2}, -\frac{1}{2})$ to $(-\frac{3}{2}, -\frac{1}{2})$ transition at 287.7 MHz and a 6-Hz shift of the $(-\frac{3}{2}, \frac{1}{2})$ to $(-\frac{5}{2}, \frac{1}{2})$ transition frequency at 286.7 MHz. For some experiments, the magnetic field was stabilized to an NMR probe. Because of the space limitations, the probe had to be located in a region where the field was not very homogeneous. This resulted in a fractional NMR linewidth of about 10^{-3} with a sample of diameter approximately 1 cm. The field fluctuations were at best about 1×10^{-6} over short time periods, as determined by the resonance linewidths. However, long-term drifts of about 10^{-5} , due primarily to changes with temperature of the tuned circuit in the NMR probe, were observed over periods of about 1 h. This field stabilization method was used to obtain the data reported previously.¹³ Another field stabilization method, based on sensing the electronic spin-flip transition of the ions, will be discussed later.

The light used for state preparation and detection causes resonances to be shifted and broadened.²⁴ These effects can be eliminated by shutting the light off while the transition is driven. When the light was chopped, the linewidth of the $(-\frac{5}{2}, -\frac{1}{2})$ to $(-\frac{3}{2}, \frac{1}{2})$ electronic spin-flip transition was observed to be as narrow as 15 kHz, which is con-

sistent with the measured short-term magnetic-field stability. The light was chopped on and off with a 50% duty cycle at a rate typically between 10 and 100 Hz. When the light was not chopped, linewidths as wide as 1.3 MHz were observed. The narrowing of the resonances when the light was chopped indicates that the transitions were driven primarily when the light was off.

The light-broadened line shape can be understood by applying the Bloch equations²⁵ to the effective two-level system consisting of the $(-\frac{5}{2}, -\frac{1}{2})$ and $(-\frac{3}{2}, \frac{1}{2})$ states. The ions spend very little time in any of the other ground-state or excited-state sublevels. In the absence of the microwave radiation, the state populations relax to their steady-state values with a time constant T_1 , which can be measured by first saturating the microwave transition, then suddenly shutting off the microwave power, and observing the fluorescence return to its normal level, as shown in Fig. 2 of Ref. 16. Typically, T_1 was about 1 s, which corresponds to an average light intensity of about 3.5 mW/cm². The transverse relaxation time T_2 was much shorter, since every optical scattering event destroyed the coherence of the effective two-level system. The resonance linewidth in the limit of zero microwave power is $1/(\pi T_2)$. This was observed to vary from about 40 kHz or less to 250 kHz, depending upon laser intensity and overlap of the light beam and ion cloud. For steady, uniform illumination $2/T_2 = \gamma_s$, where γ_s is the average scattering rate. If the overlap of the beam with the cloud is poor, then the light is effectively chopped on and off as the magnetron motion²³ takes the ions into and out of the beam. In this case, the effective scattering rate which determines T_2 saturates at about the magnetron frequency ν_m as the light intensity increases.

The resonance linewidths were observed to increase with microwave power in accordance with theory.²⁵ This increase gave an absolute calibration of the microwave magnetic field amplitude at the ions. Under typical operating conditions, this was about 2×10^{-8} T (0.2 mG). Similar light broadening effects were seen on the $(-\frac{5}{2}, -\frac{1}{2})$ to $(-\frac{3}{2}, -\frac{1}{2})$ nuclear spin-flip transition, but were not studied in detail. They were eliminated by chopping the light, so that linewidths of about 30 Hz were observed, due to magnetic-field fluctuations during the time required to sweep the resonance.

In most cases, light shifts²⁴ of resonances were difficult to observe because of field fluctuations and light broadening effects. However, in one case, a light shift was definitely observed. The $(-\frac{3}{2}, \frac{1}{2})$ to $(-\frac{1}{2}, \frac{1}{2})$ field insensitive transition at $B_0 = 1.24$ T was observed by the quadruple resonance

method described previously. This transition was driven with the light on and with it off. In both cases, the rf pulses at the $(-\frac{5}{2}, \frac{1}{2})$ to $(-\frac{3}{2}, \frac{1}{2})$ and the $(-\frac{3}{2}, \frac{1}{2})$ to $(-\frac{1}{2}, \frac{1}{2})$ transition frequencies were separated in time in order not to broaden the resonance. The resonance frequency was shifted down by about 3.5 Hz when the light was on relative to its value when the light was off. This shift implies an average light intensity of about 10 mW/cm², which is in reasonable agreement with the value inferred from T_1 .

Bloch-Siegert and other rf line-pulling effects²⁶ were negligible because of the low powers used. Line broadenings or shifts due to real or virtual transitions induced by the auxiliary rf fields in the triple and quadruple resonance methods can be eliminated by shutting them off while the main transition is driven.

E. Zeeman resonance magnetic-field stabilization

A system was developed which servoed the magnetic field by keeping the frequency of the $(-\frac{5}{2}, -\frac{1}{2})$ to $(-\frac{3}{2}, -\frac{1}{2})$ electronic spin-flip transition resonant with a fixed microwave frequency. Other rf transition frequencies were measured while the field was thus stabilized. The field stabilization scheme worked as follows: The light was tuned close to resonance with the $(^2S_{1/2}, m_I = -\frac{1}{2}, m_J = -\frac{1}{2})$ to $(^2P_{3/2}, m_I = -\frac{5}{2}, m_J = -\frac{3}{2})$ transition frequency. A microwave frequency ν , with which to stabilize the electronic spin-flip transition, was chosen. The microwave radiation was shut off for 0.2 s, so that the rf transition could be driven without broadening from this source. The ions were subjected to microwave radiation of frequency $\nu + 10$ kHz for 0.8 s. Scattered photons were counted during this period and the number was stored. The microwave radiation was shut off for 0.2 s. It was turned on again for 0.8 s at frequency $\nu - 10$ kHz and the scattered photons were counted. This number was digitally subtracted from the one stored previously. If the result was positive, the field was too low, and vice versa. This number was sent to a digital-to-analog converter which was connected to an analog integrator. The output of the integrator controlled the magnet power supply and corrected the field. The cycle was then repeated. Either the $(-\frac{5}{2}, -\frac{1}{2})$ to $(-\frac{3}{2}, -\frac{1}{2})$ or the $(-\frac{3}{2}, \frac{1}{2})$ to $(-\frac{1}{2}, \frac{1}{2})$ nuclear spin-flip transitions could be detected by a decrease in the average photon scattering rate when rf at the resonance frequency was introduced. The light was chopped at about 8 Hz to reduce light broadenings and shifts of the resonances. A typical nuclear spin-flip resonance curve is shown in Fig. 3. Unfortunately, the field stability achieved with this

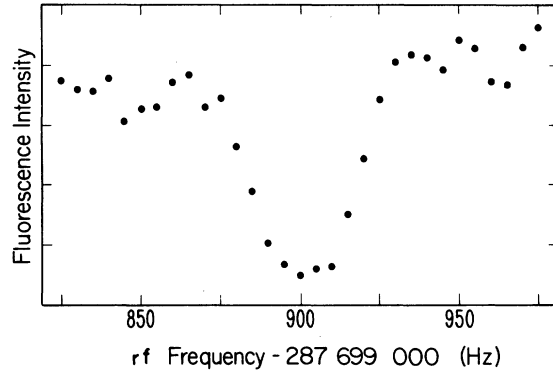


FIG. 3. rf resonance curve for the $(m_I, m_J) = (-\frac{5}{2}, -\frac{1}{2})$ to $(-\frac{3}{2}, -\frac{1}{2})$ hyperfine transition. The magnetic field B_0 was actively stabilized by keeping the $(-\frac{5}{2}, -\frac{1}{2})$ to $(-\frac{5}{2}, +\frac{1}{2})$ electronic spin-flip resonance centered at 33 466.187 MHz, which corresponds to $B_0 \cong 1.1405$ T. The 35-Hz linewidth is due primarily to the remaining short-term fractional fluctuations in B_0 of about 10^{-6} . Each point represents an integration time of 4 s.

system was limited by the low signal-to-noise ratio and the relatively poor short-term stability of the magnet. The fractional field fluctuations, estimated from the widths and reproducibility of the nuclear spin-flip resonances, were about 1×10^{-6} . These experiments were all carried out at $B_0 \cong 1.14$ T. This was experimentally convenient because the dye laser could be locked to a strong I_2 hyperfine feature.

F. Field independent transition

The first derivative with respect to the magnetic field of the $(-\frac{3}{2}, \frac{1}{2})$ to $(-\frac{1}{2}, \frac{1}{2})$ transition frequency goes to zero at a field of approximately 1.24 T. The fractional frequency shift $\delta\nu/\nu$ for a fractional field shift $\delta B/B$ from this field is $-0.012 (\delta B/B)^2$. This transition was detected by the quadruple resonance scheme outlined briefly in Sec. II C. The $(-\frac{3}{2}, -\frac{1}{2})$ to $(-\frac{1}{2}, \frac{1}{2})$ electronic spin-flip frequency for this field could be predicted from previous data with an uncertainty of less than 10^{-5} . The microwave source was set to this frequency and the magnetic field adjusted until the decrease in fluorescence corresponding to the double resonance was observed. The field was left unstabilized, but was periodically reset by this method. The drift, after warmup, was on the order of $(1-2) \times 10^{-5}$ over 30 min, so it was not a serious problem. The microwave source was frequency swept at a rate of about 8 Hz by ± 750 kHz, so that the ions would still be in resonance during part of the sweep, even if the field drifted by $\pm 2 \times 10^{-5}$. This field shift corresponds to a frequency shift $\delta\nu$ of 1.4×10^{-3} Hz on the $(-\frac{3}{2}, \frac{1}{2})$ to $(-\frac{1}{2}, \frac{1}{2})$ transition. The necessary dye laser fre-

quency for this field was about 25 MHz away from the nearest hyperfine feature in I_2 . The laser frequency was stabilized to this feature by frequency shifting part of the beam by 25 MHz with an acousto-optic modulator and passing it through the I_2 cell.

The measurement sequence was as follows: The microwave source was left on continuously. We estimate that this caused an rf Stark shift of the $(-\frac{3}{2}, \frac{1}{2})$ to $(-\frac{1}{2}, \frac{1}{2})$ transition frequency of less than 10^{-4} Hz. The light was then blocked with an electromechanical shutter to eliminate light shifts and broadenings. An rf oscillator was switched on for a period of about 1 s to drive the $(-\frac{5}{2}, \frac{1}{2})$ to $(-\frac{3}{2}, \frac{1}{2})$ transition. The oscillator was frequency modulated by about 600 Hz at a rate of about 9 Hz to eliminate any sensitivity to field drifts. After this first rf oscillator was shut off, the $(-\frac{3}{2}, \frac{1}{2})$ to $(-\frac{1}{2}, \frac{1}{2})$ transition was then driven. Both the Rabi single-pulse method and the Ramsey two-pulse method were used.²⁷ For the Rabi method, the rf was switched on for a period t . For the Ramsey method, the rf was turned on for a period τ , off for a period T , and on again for a period τ . The two pulses were coherent in phase because the oscillator ran continuously during the period T , but was attenuated by 130 dB. At the end of this resonance period, the first rf oscillator was switched on for about 1 s to drive the $(-\frac{5}{2}, \frac{1}{2})$ to $(-\frac{3}{2}, \frac{1}{2})$ transition. The light was then unblocked and the scattered photons were counted. The initial fluorescence level was lower if ions had been driven to the $(-\frac{1}{2}, \frac{1}{2})$ level, than if they had not. The fluorescence level then rose to the previous steady-state value as the ions were optically pumped.¹⁷ The initial fluorescence level (first 2 to 4 s) was divided by the final level (next 4 to 10 s) in order to obtain a signal that was less sensitive to long-term laser intensity fluctuations. This cycle was repeated several times for each frequency setting of the $(-\frac{3}{2}, \frac{1}{2})$ to $(-\frac{1}{2}, \frac{1}{2})$ rf oscillator in order to improve the signal-to-noise ratio.

With the Rabi method, one obtains a linewidth (in Hz) of $(1.25t)^{-1}$ at optimum rf power. Linewidths as small as 40 mHz were observed with $t = 20$ s. With the Ramsey method with $\tau \ll T$ and optimum rf power, one obtains an oscillating line shape with a central minimum of width of $(2T)^{-1}$. The central minimum can be identified by the fact that it does not change for different T or by using the Rabi method, which yields only one deep minimum. Linewidths as small as 12 mHz were observed with $T = 41.4$ s. Since the frequency was about 292 MHz, this corresponds to a Q of 2.4×10^{10} . Typical curves are shown in Figs. 4 and 5. No evidence was seen for re-

laxations between ground-state sublevels, even for these long values of T . However, the initial scattering rate (and hence, the signal) became low for $T \gtrsim 40$ s due to heating of the ions while the light was off, which increased the Doppler width.

III. RESULTS

The transition frequencies between (m_I, m_J) sublevels are given in closed form by the Breit-Rabi formula.²⁷ There are only three independent parameters in this formula: A , g_I/g_J , and $g_J\mu_B B_0/h$, where μ_B is the Bohr magneton and B_0 is the magnetic field. Hence, it is sufficient to measure three different transition frequencies at the same magnetic field to determine all three parameters. In order to decorrelate the three parameters, it is helpful to measure one $\Delta m_I = 0$, $\Delta m_J = \pm 1$ transition frequency, which depends mostly on $g_J\mu_B B_0/h$, and two $\Delta m_I = \pm 1$, $\Delta m_J = 0$ transition frequencies, which depend primarily on A and secondarily on the other parameters. One of the two $\Delta m_I = \pm 1$, $\Delta m_J = 0$ transitions should have $m_J = -\frac{1}{2}$ and the other should have $m_J = \frac{1}{2}$ in order to decorrelate A and g_I/g_J . The absolute g factors can be determined if an independent measurement of magnetic field (actually

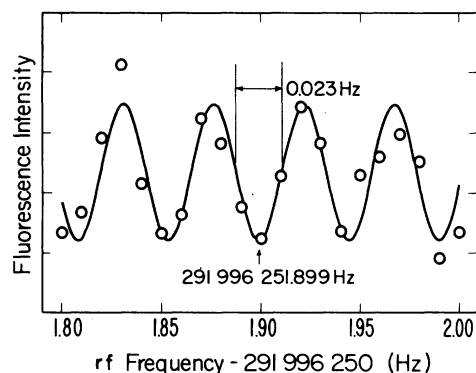


FIG. 4. rf resonance curve for the $(m_I, m_J) = (-\frac{3}{2}, \frac{1}{2})$ to $(-\frac{1}{2}, \frac{1}{2})$ hyperfine transition. Each circle represents the average of four measurements (total detection fluorescence integration time of 8 s). The solid curve is a theoretical fit. The quadrupole resonance technique described in the text was used. The oscillatory line shape results from the use of the Ramsey method to drive the transition. Two coherent rf pulses of duration $\tau = 1.02$ s separated by $T = 20.72$ s were applied. The vertical arrow marks the central minimum, which corresponds to the resonance frequency. The magnetic field B_0 was set so that the $(-\frac{5}{2}, -\frac{1}{2})$ to $(-\frac{3}{2}, -\frac{1}{2})$ electronic spin-flip resonance was in the range of $36\,248.374 \pm 0.750$ MHz, which corresponds to $B_0 \approx 1.2398$ T.

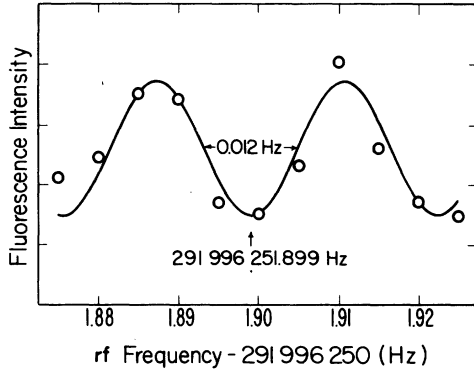


FIG. 5. rf resonance curve for the $(m_I, m_J) = (-\frac{3}{2}, \frac{1}{2})$ to $(-\frac{1}{2}, \frac{1}{2})$ hyperfine transition. Each circle represents the average of four measurements (total detection fluorescence integration time of 16 s). The pulse separation time T was 41.40 s. The experimental conditions were otherwise the same as for the curve shown in Fig. 4. The vertical arrow marks the central minimum.

$\mu_B B_0/h$ is made at the same time. However, this was not done.

At the time of our first experiments, the value of A was not very well known.^{5,16,28} The $^{25}\text{Mg}^+$ $(-\frac{5}{2}, -\frac{1}{2})$ to $(-\frac{3}{2}, \frac{1}{2})$ transition was found after searching a frequency range corresponding to A values from -628 to -595 MHz. The value of $g_J \mu_B B_0/h$ had been determined from the electronic spin-flip transition frequency of $^{24}\text{Mg}^+$, before loading $^{25}\text{Mg}^+$ into the trap. After allowing for drift of the magnetic field between measurements, A could be determined with a fractional uncertainty of 2×10^{-3} by taking g_I from previous NMR measurements and assuming g_J was equal to the free-electron g factor.

The positions of the other transitions could then be predicted and were observed by the methods described previously. Several transition frequencies were measured at each of several magnetic-field settings between 1.0 and 1.2 T, and were used to determine A and g_I/g_J .¹³

Our final determinations of A and g_I/g_J are based on a combination of the $(-\frac{5}{2}, -\frac{1}{2})$ to $(-\frac{3}{2}, -\frac{1}{2})$ transition frequency measured with the Zeeman resonance field stabilization scheme at magnetic field $B(1)$ and the $(-\frac{3}{2}, \frac{1}{2})$ to $(-\frac{1}{2}, \frac{1}{2})$ field-independent transition frequency at magnetic field $B(2)$. There are thus four parameters to be determined: A , g_I/g_J , $g_J \mu_B B(1)/h$, and $g_J \mu_B B(2)/h$. Four independent equations are provided by the Breit-Rabi formula expressions for the four frequencies $\nu(1)$ through $\nu(4)$. Here $\nu(1)$ and $\nu(2)$ are, respectively, the $(-\frac{5}{2}, -\frac{1}{2})$ to $(-\frac{3}{2}, \frac{1}{2})$ and the $(-\frac{5}{2}, -\frac{1}{2})$ to $(-\frac{3}{2}, -\frac{1}{2})$ transition frequencies at $B(1)$ and $\nu(3)$ and $\nu(4)$ are, respectively, the $(-\frac{5}{2},$

$-\frac{1}{2})$ to $(-\frac{3}{2}, \frac{1}{2})$ and the $(-\frac{3}{2}, \frac{1}{2})$ to $(-\frac{1}{2}, \frac{1}{2})$ transition frequencies at $B(2)$. The experimental results (in MHz) are

$$\begin{aligned} \nu(1) &= 33\,466.187\,13, \\ \nu(2) &= 287.699\,897(48), \\ \nu(3) &= 36\,248.374, \\ \nu(4) &= 291.996\,251\,899(3). \end{aligned} \quad (1)$$

No uncertainty is shown for $\nu(1)$ or $\nu(3)$, since they were fixed experimentally. [Uncertainties in $\nu(1)$ or $\nu(3)$ due to magnetic-field fluctuations would show up as fluctuations in $\nu(2)$ or $\nu(4)$, respectively.] The uncertainty of $\nu(2)$ due to the lack of reproducibility of the line centers from run to run was only about 19 Hz. The uncertainty of $\nu(2)$ has been increased to reflect possible offsets of the field servo system due to light shifts of the electronic spin-flip transition frequency or to the magnetic-field inhomogeneity. These effects were reduced by chopping the light, but may not have been completely eliminated, because the microwave power and the light were not chopped alternately. Thus, the microwave resonance line shapes may have consisted of a broad, shifted component, due to transitions made while the light was on, and a narrow, unshifted component due to transitions made while the light was off. The microwave power was adjusted so that the linewidths were about 40 kHz, due largely, if not totally, to short-term field fluctuations. We estimate that the offset from the light-shifted component should have caused a fractional shift in the field of less than 10^{-6} , which would cause a shift in $\nu(2)$ of less than 16 Hz. The field inhomogeneity over a typical ion cloud diameter of about 150 μm is estimated to be less than 3×10^{-6} , and to a high degree the effect on the resonances is averaged away as the individual ions circulate through the volume. A direct light shift of the $\nu(2)$ resonance would be accompanied by a broadening of several kHz, which we did not observe. No uncertainty is shown for $\nu(3)$, which was swept by ± 750 kHz around this center value. The uncertainty shown for $\nu(4)$ reflects, in about equal parts, the statistical uncertainty of determining the line center and possible magnetic-field drift within the limits set by the frequency modulation of $\nu(3)$. The results of the fit are

$$\begin{aligned} A &= -596.254\,376(54) \text{ MHz}, \\ g_I/g_J &= 9.299\,484(75) \times 10^{-5}. \end{aligned} \quad (2)$$

These results are in agreement with, and about a factor of 4 more precise than our previously reported values. Essentially all of the uncertainty of the fit is due to the uncertainty of $\nu(2)$. Also

determined were $g_J \mu_B B(1)/h = 31\,962.151\,585$ MHz and $g_J \mu_B B(2)/h = 34\,745.375\,447$ MHz. The corresponding value of the magnetic field at the position of the ions in terms of its value at the position of the NMR probe was not known very precisely. Hence, we are only able to say that g_J is approximately equal to the g value of the free electron g_e , e.g., $g_J = 2.002(2)$.

We have estimated that all perturbations to A and g_I/g_J , such as pressure, Stark, and diamagnetic shifts are negligible compared to the stated uncertainties. If the diamagnetic shift of A has a coefficient comparable to the measured value for ^{85}Rb ,²⁹ then its contribution to $\nu(4)$ is around 0.3 Hz, which is much greater than the uncertainty of $\nu(4)$. However, this does not affect the determinations of A and g_I/g_J , since their uncertainties are dominated by the uncertainty of $\nu(2)$.

IV. DISCUSSION

The present result for A is generally in agreement with the previous less precise measurements. An observation of the $3s\,^2S_{1/2}$ to $3p\,^2P_{3/2}$ resonance line has been made by Crawford *et al.*, using an atomic beam source and Fabry-Perot etalons.²⁸ Their reported value for A is $-693(38)$ MHz, which differs from ours by 16%. The only other reported optical measurement of A is that of Drullinger *et al.*,¹⁶ using the method of laser fluorescence, stored ion spectroscopy. The isotope shifts and hyperfine structure of the $(3s\,^2S_{1/2}, m_J = -\frac{1}{2})$ to $(3p\,^2P_{3/2}, m_J = -\frac{3}{2})$ Zeeman component in a magnetic field of about 0.98 T were observed. The value obtained was $A = -608(50)$ MHz, in good agreement with the present result. Both of the optical determinations depend on assumptions about the isotope shift (the mass-shift formula is assumed) and on an estimate of the $^2P_{3/2}$ hyperfine structure. However, the uncertainties of these effects are small compared with the experimental precision. Weber and Grägel⁵ measured A by optical pumping in a buffer-gas cell. Their result, $A = -616(50)$ MHz, is in good agreement with the present result. Brom and Weltner⁸ have observed the electron spin resonance (ESR) spectrum of $^{25}\text{Mg}^+$ trapped in a solid argon matrix at 4 K. Their result was $A = -595.0(3)$ MHz, which indicates that A is reduced by 0.21(5)% under these conditions relative to its free-ion value (present determination). This is less than typical shifts for alkali atoms under similar conditions.¹⁰

Ab initio calculations of A in $^{25}\text{Mg}^+$ should be possible with about the same accuracy as for ^{23}Na ,³⁰ since the two systems are isoelectronic.

The only such calculation that has been carried out so far is by Lindgren,³¹ who obtains $A = -456$ MHz in the restricted Hartree-Fock approximation (-463 MHz with relativistic corrections) and $A = -545$ MHz when core polarization is included (-553 MHz with relativistic corrections). The remaining 7% difference between the relativistic calculation including core polarization and the experimental result is presumably due to pure correlation effects involving double excitations.

The semiempirical Fermi-Segrè formula^{19,32} predicts $A = -627.8$ MHz, which is 5% too high in magnitude. The NMR measurement of g_I ,²¹ uncorrected for diamagnetic effects, is used. Relativistic correction factors are left out. The derivative of the quantum defect with respect to quantum number which appears in this formula was evaluated from the extended Ritz formula given by Risberg.²⁰ If this term is left out, leaving the Goudsmit formula, the result ($A = -606.4$ MHz) is actually in better agreement with experiment.

Veseth has carried out a Hartree-Fock calculation of g_J of Mg^+ .³³ The values obtained for the individual correction terms, in the notation of Ref. 34, are $\delta_2 = -7.91 \times 10^{-5}$, $\delta_3 = 9.70 \times 10^{-5}$, and $\delta_4 = -7.66 \times 10^{-5}$. The final result is $g_J = 2.002\,260\,6$, with an estimated fractional uncertainty of 3×10^{-6} .

Hegstrom, using a simple hydrogenic approximation for the valence electron, obtains $g_J/g_e = (1-31) \times 10^{-6}$, or $g_J = 2.002\,257$.³⁵ The g_J value of $^{25}\text{Mg}^+$ trapped in a solid argon matrix at 4 K was reported by Brom and Weltner⁸ to be 2.006(4). The shift from the free-ion value is consistent with theory.

Our result for g_I/g_J can be combined with Veseth's calculated value of g_J to obtain g_I for the free $^{25}\text{Mg}^+$ ion. This can be combined with the NMR result for g_I of $^{25}\text{Mg}^{2+}$ ions in H_2O (Ref. 21) to obtain the shielding difference

$$\sigma^* = 1 - g_I(\text{NMR})/g_I(\text{free ion})$$

$$= -9.9(9) \times 10^{-5}.$$

The corresponding shielding differences for the alkali atoms (free atoms versus hydrated ions) have been measured.³⁶ They also are negative and increase monotonically in magnitude with atomic number Z . For ^{23}Na , $\sigma^* = -6.05(10) \times 10^{-5}$.

The absolute accuracy of our measurements could, of course, be substantially improved if the magnetic-field stability and homogeneity were improved. Accurate measurements of g_J could be made by comparing the electronic spin-flip frequency in the ion, $g_J \mu_B B_0/h$, to, for example, the cyclotron frequency of free electrons,³⁷ $2\mu_B B_0/h$.

h , in the same magnetic field.

These same experimental techniques could be extended to measure hyperfine constants and g factors of other ions,³⁸ such as $^9\text{Be}^+$. The high resolution with small perturbations which can be obtained may make it possible to study small effects not previously observed, such as the diamagnetic susceptibility of the nucleus,²⁹ or to realize new types of frequency standards.

ACKNOWLEDGMENTS

We wish to thank J. C. Bergquist and R. E. Drullinger for experimental assistance during the early part of the work. This work was supported in part by the Air Force Office of Scientific Research and the Office of Naval Research. One of us (W.M.I.) acknowledges the financial support of the NRC in the form of a Postdoctoral Research Associateship during this work.

- ¹For reviews, see E. Arimondo, M. Inguscio, and P. Violino, *Rev. Mod. Phys.* **49**, 31 (1977); G. H. Fuller, *J. Chem. Phys. Ref. Data* **5**, 835 (1976).
- ²For recent work on radioactive alkalis, including francium, see S. Liberman, J. Pinard, H. T. Duong, P. Juncar, P. Pillet, J.-L. Vialle, P. Jacquinot, F. Touchard, S. Büttgenbach, C. Thibault, M. de Saint-Simon, R. Klapisch, A. Pesnelle, and G. Huber, *Phys. Rev. A* **22**, 2732 (1980) and references therein.
- ³For examples of recent work and reviews, see M. Vajed-Samii, S. N. Ray, T. P. Das, and J. Andriessen, *Phys. Rev. A* **20**, 1787 (1979); S. Garpman, I. Lindgren, J. Lindgren, and J. Morrison, *Z. Phys. A* **276**, 176 (1976); I. Lindgren, *Phys. Scr.* **11**, 111 (1975).
- ⁴For a review, see E. W. Weber, *Phys. Rep.* **32**, 123 (1977).
- ⁵E. W. Weber and R. Grägel, private communication.
- ⁶F. G. Major and G. Werth, *Phys. Rev. Lett.* **30**, 1155 (1973); *Appl. Phys.* **15**, 201 (1978); M. D. McGuire, R. Petsch, and G. Werth, *Phys. Rev. A* **17**, 1999 (1978).
- ⁷R. Blatt and G. Werth, *Z. Phys. A* **299**, 93 (1981).
- ⁸J. M. Brom and W. Weltner, *J. Chem. Phys.* **58**, 5322 (1973).
- ⁹P. H. Kasai, *Phys. Rev. Lett.* **21**, 67 (1968).
- ¹⁰C. K. Jen, V. A. Bowers, E. L. Cochran, and S. N. Foner, *Phys. Rev.* **126**, 1749 (1962).
- ¹¹W. L. Randolph, J. Asher, J. W. Koen, P. Rowe, and E. Matthias, *Hyper. Interact.* **1**, 145 (1975).
- ¹²J. Hata and M. Sakai, *Phys. Lett.* **57A**, 419 (1976); S. N. Ray, J. E. Rodgers, and T. P. Das, *Phys. Rev. A* **13**, 1983 (1976); S. Ahmad, J. Andriessen, K. Raghunathan, and T. P. Das, *Bull. Am. Phys. Soc.* **26**, 481 (1981).
- ¹³W. M. Itano, D. J. Wineland, R. E. Drullinger, and J. C. Bergquist, Abstracts of the 7th International Conference on Atomic Physics, MIT, Cambridge, 1980 (unpublished), p. 238.
- ¹⁴W. Neuhauser, M. Hohenstatt, P. E. Toschek, and H. Dehmelt, *Phys. Rev. Lett.* **41**, 233 (1978); *Appl. Phys.* **17**, 123 (1978); *Phys. Rev. A* **22**, 1137 (1980).
- ¹⁵D. J. Wineland, R. E. Drullinger, and F. L. Walls, *Phys. Rev. Lett.* **40**, 1639 (1978).
- ¹⁶R. E. Drullinger, D. J. Wineland, and J. C. Bergquist, *Appl. Phys.* **22**, 365 (1980).
- ¹⁷D. J. Wineland, J. C. Bergquist, W. M. Itano, and R. E. Drullinger, *Opt. Lett.* **5**, 245 (1980).
- ¹⁸D. J. Wineland and W. M. Itano, *Phys. Lett.* **82A**, 75 (1981).
- ¹⁹H. Kopfermann, *Nuclear Moments* (Academic, New York, 1958).
- ²⁰P. Risberg, *Ark. Fys.* **9**, 483 (1955).
- ²¹O. Lutz, A. Schwenk, and A. Uhl, *Z. Naturforsch.* **30a**, 1122 (1975).
- ²²A. Lurio, *Phys. Rev.* **126**, 1768 (1962); J. Bauche, G. Couarraze, and J.-J. Labarthe, *Z. Phys.* **270**, 311 (1974).
- ²³H. Dehmelt, in *Advances in Atomic and Molecular Physics*, edited by D. R. Bates and I. Estermann (Academic, New York, 1967, 1969), Vols. 3 and 5.
- ²⁴W. Happer, *Rev. Mod. Phys.* **44**, 169 (1972).
- ²⁵A. Abragam, *The Principles of Nuclear Magnetism* (Oxford University Press, London, 1961).
- ²⁶M. Mizushima, *Phys. Rev.* **133**, A414 (1964).
- ²⁷N. F. Ramsey, *Molecular Beams* (Oxford University Press, London, 1956).
- ²⁸M. F. Crawford, F. M. Kelly, A. L. Schawlow, and W. M. Gray, *Phys. Rev.* **76**, 1527 (1949).
- ²⁹N. P. Economou, S. J. Lipson, and D. J. Larson, *Phys. Rev. Lett.* **38**, 1394 (1977).
- ³⁰T. Lee, N. C. Dutta, and T. P. Das, *Phys. Rev. A* **1**, 995 (1970).
- ³¹I. Lindgren, private communication.
- ³²L. L. Foldy, *Phys. Rev.* **111**, 1093 (1958).
- ³³L. Veseth, private communication.
- ³⁴L. Veseth, *Phys. Rev. A* **22**, 803 (1980).
- ³⁵R. Hegstrom, private communication.
- ³⁶A. Beckmann, K. D. Böklen, and D. Elke, *Z. Phys.* **270**, 173 (1974).
- ³⁷See for example, H. G. Dehmelt and F. L. Walls, *Phys. Rev. Lett.* **21**, 127 (1968); R. M. Jopson and D. J. Larson, *Bull. Am. Phys. Soc.* **25**, 1133 (1980).
- ³⁸W. M. Itano and D. J. Wineland, *Bull. Am. Phys. Soc.* **24**, 1185 (1979).